Deuteron Magnetic Dipole Disintegration by 180° Electron Scattering*

G. A. PETERSON† AND W. C. BARBER
High-Energy Physics Laboratory, Stanford University, Stanford, California
(Received May 31, 1962)

The magnetic dipole disintegration of the deuteron has been measured for excitation energies up to 16 MeV in the presence of relatively small electric multipole contributions by using a method of inelastic electron scattering at 180°. Electrons of initial energy 41.5 MeV were magnetically deflected before and after scattering so that those scattered at 180° entered a magnetic spectrometer set at 160° with respect to the incident beam. The experimental cross sections measured relative to elastic scattering from the proton are higher than predicted by the electrodisintegration theory of Jankus. The discrepancy may be an indicati on of mesonic exchange currents which are not included in the Jankus theory.

I. INTRODUCTION

THE magnetic dipole disintegration of the deuteron involves an interaction of an electromagnetic field with the current and magnetization densities of the deuteron. The shape and magnitude of the cross section may depend not only on currents due to nucleon motions, but upon exchange currents, which arise in the theory from the introduction of a space exchange operator in the nucleon-nucleon coupling, and which depend on the detailed nature of the meson field.

In low-energy deuteron photodisintegration the electric dipole disintegration ($E1$) dominates over the magnetic dipole disintegration ($M1$) except near threshold. In principle, a separation of $E1$ from $M1$ can be made by measuring the angular distribution of protons or neutrons. However, $E1$ dominates over $M1$ so strongly that it is difficult to make the separation for excitation energies greater than about 1 MeV.[1,2]

In deuteron electrodisintegration it is possible to suppress $E1$ with respect to $M1$ by a proper choice of scattering kinematics. By detecting electrons scattered inelastically into the far backward direction, one can observe $M1$ in the presence of relatively small electric multipole contributions.

The relative importance of various multipole transitions for electron scattering may be estimated in the virtual photon approximation[3] which relates electron- to photon-induced cross sections. If an electron scatters through 180°, the ratio of $M1$ to $E1$ electron scattering cross sections, for equal $E1$ and $M1$ photodisintegration cross sections, is given by $R \simeq [(p_0+p)/(p_0-p)]^2$, where p_0 and p are the electron's momenta before and after scattering. Large values of R may result. For example, for a deuteron excitation energy of 1 MeV and $p_0c=41.5$ MeV, $R=260$.

Furthermore, elastic electron scattering is minimized at 180° together with the electron spectrum resulting from elastic scattering accompanied by radiation. This spectrum, sometimes referred to as the "radiation tail," presents a severe background problem in low-energy inelastic electron scattering experiments ($E_0 \lesssim 100$ MeV). Measurements must be restricted to the backward angles where inelastic scattering from nuclear levels can be observed above the radiation tail background.[3] The reduction of the radiation tail by 180° scattering makes possible the investigation of low-energy magnetic-multipole transitions[4] which would be difficult at other angles.

This paper describes the apparatus and methods of 180° electron scattering, and the results of inelastic scattering from the deuteron for excitation energies up to 16 MeV. The deuteron data are normalized to the elastic scattering from the proton in order to obtain experimental electrodisintegration cross sections. We assume the validity of the theoretical electron-proton cross section of Rosenbluth,[5] modified by form factors. The results are compared with the electrodisintegration theory of Jankus.[6]

II. EXPERIMENTAL APPARATUS

An electron beam from the Stanford Mark II linear accelerator was deflected in a two-magnet achromatic translation system.[7] The field of the first (momentum analyzing) magnet of this system was monitored with a nuclear resonance water probe and an associated wide-range oscillator.[8] The time-integrated beam current was measured with a three-foil secondary-emission monitor and an electronic "slide-back" integrator. Systematic errors of beam monitoring were avoided by taking all data for the same incident electron energy, $E_0=41.5$ MeV, and beam current, 0.4 μA.

After the beam passed through the secondary emission monitor, it entered a Lucite vacuum chamber situated between the rectangular pole pieces of a small magnet, as shown in Fig. 1. This magnet deflected the

* This work was supported by the joint program of the Office of Naval Research, the U. S. Atomic Energy Commission, and the Air Force Office of Scientific Research.
† Present address: Yale University, New Haven, Connecticut.
[1] G. R. Bishop, L. E. Beghian, and H. Halban, Phys. Rev. **83**, 1052 (1951).
[2] W. M. Woodward and I. Halpern, Phys. Rev. **76**, 107 (1949).
[3] W. C. Barber, F. Berthold, G. Fricke, and F. E. Gudden, Phys. Rev. **120**, 2081 (1960); and R. H. Dalitz and D. R. Yennie, *ibid.* **105**, 1598 (1957).
[4] R. Edge and G. Peterson, Phys. Rev. (to be published).
[5] N. M. Rosenbluth, Phys. Rev. **79**, 615 (1950); and R. Hofstadter, Ann. Rev. Nuclear Sci. **7**, 231 (1957).
[6] V. Z. Jankus, Phys. Rev. **102**, 1586 (1956).
[7] K. L. Brown, Rev. Sci. Instr. **27**, 959 (1956).
[8] L. Buss and L. Bogart, Rev. Sci. Instr. **31**, 204 (1960).

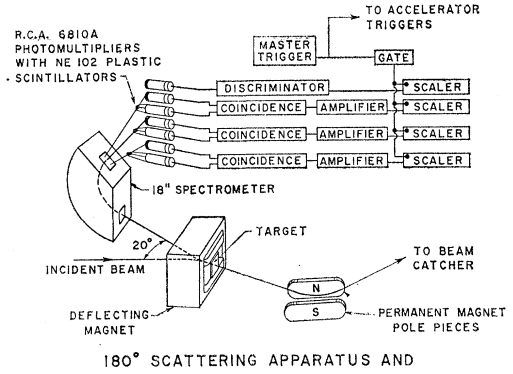

FIG. 1. Experimental arrangement for 180° electron scattering.

beam less than 10° before it struck a target located in air at a position where the fringing field was 5% of the maximum field value. Electrons scattered at 180° re-entered the magnetic field approximately perpendicular to the longer edges of the pole pieces and were deflected so that the total deflection of the incoming and scattered electrons was 20°. Mappings of the magnetic field indicated that the field was uniform parallel to the longer edges of the pole pieces and that the ratio of the vertical deflecting to the horizontal focusing field was large. The incident beam was 0.6 cm high and the pole pieces were separated 5.3 cm.

Distortions of the incident and scattered beams, either through focusing or defocusing, were small for this simple and symmetrical beam deflection method. Beyond the target a large permanent magnet deflected the beam upward, as shown in Fig. 1, and thus largely eliminated background scattering.

In this manner electrons scattered from the target at 180° were deflected into a double-focusing, 120°, 18-in. radius, magnetic spectrometer set at 160° with respect to the incident beam. The magnetic field of this spectrometer was monitored directly with a precision rotating coil designed by Bumiller.[9]

The electrons were detected by three double-coincidence counter telescopes consisting of RCA 6810A photomultipliers with 1.3-mm plastic scintillators mounted parallel to the photocathodes. The photomultiplier pulses were sent directly into coincidence circuits[10] set for 5-nsec resolution. A singles counter was used to monitor background. The photomultipliers were glued into the spectrometer vacuum system at the rim of the projecting metal to glass seal. One photomultiplier of each counter telescope was mounted on an expansible vacuum bellows. This arrangement permitted alignment of the scintillators by alpha-particle counting so that when they were properly aligned, an unscattered electron which traversed the center of the first scintillator, 2.5 cm high, would strike the center of the second scintillator, 4.5 cm in diam. Care in alignment was necessary because electrons multiply scatter in the first scintillator and a fraction of them miss the second scintillator. A calculation of these energy-dependent counting losses with the multiple scattering theory of Scott[11] showed that they were less than 8% in all channels for even the lowest energy electron observed in this experiment. Corrections were made in analyzing the data.

The rotating coil spectrometer monitor was calibrated at one field setting of the spectrometer by counting Cm^{244} alpha particles in each of the three counter telescopes.

III. EXPERIMENTAL METHOD

In order to find the correct field B_0 of the small deflecting magnet corresponding to 180° elastic scattering, use was made of the angular dependence of elastic scattering. The elastic scattering through an angle θ of electrons of energy E_0 by nuclei of low atomic number Z without spin is described by the Mott formula modified by a form factor $F(q)$:

$$\frac{d\sigma}{d\Omega}=\left(\frac{d\sigma}{d\Omega}\right)_{\text{Mott}}|F(q)|^2$$

$$=\left(\frac{Ze^2}{2E_0}\right)^2\left[\frac{\csc^4(\theta/2)}{1+(2E_0/Mc^2)\sin^2(\theta/2)}\right]$$

$$\times\left(\frac{m^2c^4}{2E_0^2}+\frac{1+\cos\theta}{2}\right)|F(q)|^2. \quad (1)$$

A minimum in the scattering is predicted for $\theta=180°$. The field of the small deflecting magnet was varied in order to find a field B_0 corresponding to the minimum elastic peak height for carbon, as shown in Fig. 2.[12] Since the spectrometer was set at 160° with respect to the incident beam, the incident beam and the scattered beam were each deflected 10°, if we do not consider the recoil of the nucleus.

A simple equation was developed for the correct field B for inelastic scattering. It was assumed that the field was uniform and that all electrons traveled the same path length s in the field. The deflection d_i of an incident electron of momentum p_0 at a radius ρ_i is

$$d_i(B,p_0)=\frac{S}{\rho_i}=\frac{B}{B_0}\times 10°.$$

[9] F. A. Bumiller, Rev. Sci. Instr. (to be published).

[10] A. Barna, J. H. Marshall, and M. Sands, Nuclear Instr. and Methods 7, 124 (1960).

[11] W. Scott, Phys. Rev. 85, 245 (1952).

[12] If the small term $m^2c^4/2E_0^2$ is neglected in Eq. (1), $d\sigma/d\Omega=0$ at 180°. The vanishing of the cross section at 180° is a consequence of the conservation of angular momentum and helicity (to the order of $v/c\approx 1$), since an electron cannot scatter through an angle of 180° from a spin zero nucleus and at the same time conserve angular momentum and helicity. However, in an actual experiment a finite solid angle must be used. The average angle within this solid angle is less than 180°, and hence, an elastic scattering peak will be observed, even for spinless nuclei.

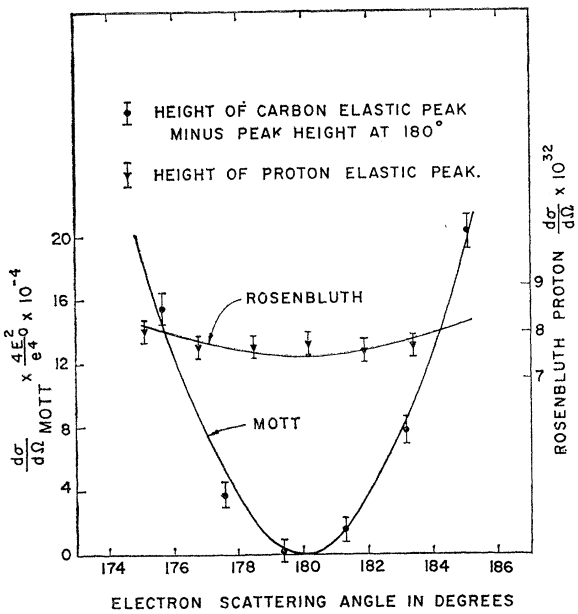

FIG. 2. Angular distribution of electrons scattered elastically from carbon nuclei and from protons near 180°. The curves are calculated from the Mott and Rosenbluth formulas and are fitted to the carbon and proton data, respectively.

The deflection of a scattered electron of momentum p is

$$d_s(B,p_0)=\frac{S}{\rho_s}=\frac{p_0B}{pB_0}\times 10^\circ.$$

The total deflection is $d_i+d_s=20°$. Hence,

$$B=2pB_0/(p+p_0). \tag{2}$$

Since B_0 was determined experimentally, a value of B corresponding to p could be found.

Equation (2) is accurate for p near p_0, that is, for low excitation energies where the virtual photon spectra for electric multipole transitions are rapidly varying functions of angle. At high excitation energies all virtual photon spectra are slowly varying functions of angle, and hence it is less important to have an accurate value of the scattering angle. For all excitation energies, the virtual photon spectra for magnetic multipole transitions are slowly varying function of angle.

If a nucleus has a spin, scattering by the magnetic moment becomes important at 180°. For example, the Rosenbluth[5] cross section describes the scattering from a proton,

$$\frac{d\sigma}{d\Omega}=\left(\frac{d\sigma}{d\Omega}\right)_{\text{Mott}}\left\{F_1^2+\frac{\hbar^2q^2}{4M^2c^2}\times[2(F_1+KF_2)^2\tan^2(\theta/2)+K^2F_2^2]\right\}, \tag{3}$$

where F_1 is the Dirac form factor, F_2 is the Pauli form factor, Mc^2 is the proton's rest energy, K is the Pauli anomalous magnetic moment, and $\hbar q$ is the four-momentum transfer. An examination of this cross section shows that it is only weakly dependent on E_0 and θ for the far backward angles near 180°. Figure 2 shows the angular dependence of the scattering from the proton for the far backward angles. The magnetic-moment elastic scattering from the proton is easily measured at 180° and it is convenient to compare other measurements to such a relatively constant and well-known[13] cross section.

Figures 3 and 4 show the scattering from a 0.153-g/cm² CH_2 target at 160° and 180°, respectively, as recorded by the middle counter telescope. About 50% of the elastic peak height labeled C of Fig. 4 is due to scattering from windows and air before and after the target. According to Eq. (3), the electron-proton scattering cross section is smaller by a factor of 2.2 at 180° than at 160°. By comparing the proton peak height to the carbon peak height, we concluded that the elastic scattering from carbon into the solid angle around 180° was a factor of 50 smaller than at 160° for approximately the same solid angle. The reduction expected from Eq. (1) was 84. The difference arises from multiple scattering contributions from angles outside of the spectrometer acceptance angle φ_m, thus effectively increasing it to some value φ_m'. An estimate of multiple scattering contributions was made by noting that for $\theta\approx 180°$, and $\varphi=180-\theta$, $(d\sigma/d\Omega)_{\text{Mott}}$ is proportional to φ^2, and hence $\int_0^{\varphi_m}(d\sigma/d\Omega)_{\text{Mott}}d\Omega\propto\varphi_m^4$.

If φ_m' includes multiple scattering, $(\varphi_m'/\varphi_m)^4\simeq 84/50$. The average backscattering angle is approximately $\frac{2}{3}\varphi_m'$. The average scattering angle, including multiple scattering, was estimated to be 177.1° from the known value of φ_m, 3.2°. This takes into account that electrons scattered at slightly different angles were received by the three counter telescopes for one setting of the deflection magnet. A more detailed estimate was unnecessary.

Figure 5 shows the results for 180° electron scattering from a 0.162-g/cm² CD_2 and a 0.124-g/cm² C (graphite)

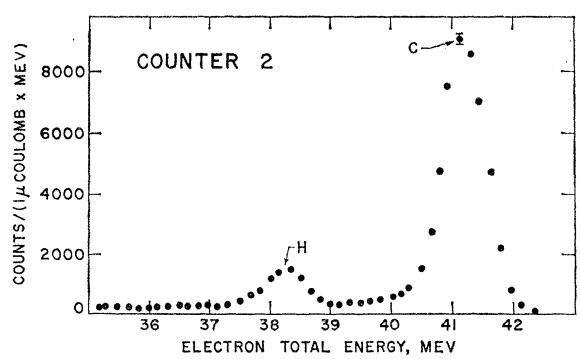

FIG. 3. Energy distribution of electrons, which were initially 41.5 MeV, after scattering through 160° from a CH_2 target.

[13] F. Bumiller, M. Croissiaux, E. Dally, and R. Hofstadter, Phys. Rev. 124, 1623 (1961).

target in the upper counter telescope. This is about one-fifth of the data used in evaluating the inelastic deuteron cross section. The peak appearing at $E=39.5$ MeV in the CD_2 data is due to elastic scattering from the deuteron. This is much smaller than the proton elastic peak of Fig. 4, even though the deuteron and the proton have the same charge, because magnetic scattering dominates at this angle and is proportional to the square of the magnetic moment of the bombarded nucleus.[14] The sharp rise at 37 MeV is the onset of the magnetic dipole disintegration of the deuteron. The only peak due to excitation of the carbon was that appearing at 26 MeV, resulting from inelastic scattering from the 15.1-MeV level. The several high points at 38 MeV appeared in every run and were attributed to a 2% contamination of hydrogen. A run at $E_0=30.5$ MeV, where the recoil energies are different, also showed a few high points where the proton peak is expected.

All points shown in Fig. 5 have been corrected for counting losses, target ionization loss differences, and variation of spectrometer "window width" to give the number of electrons at a certain energy per unit energy interval. The background with the target removed from the beam was not measured, but it was expected to be equal for the CD_2 and carbon targets. The solid target CD_2-C and CH_2-C subtractions effectively accounted for the background as well as multiple scattering contributions from larger angles. A check on the latter feature was made by varying the CH_2 target thickness for $E=23.3$ MeV for $E_0=41.5$ MeV. A linear dependence of counting rate on target thickness was found over a range of thicknesses from 0.1 to 0.3 g/cm^2. A nonlinear dependence is expected if multiple scattering contributions from larger angles are appreciable, or if thick target radiation corrections are important.

Consistency checks were made by comparing the

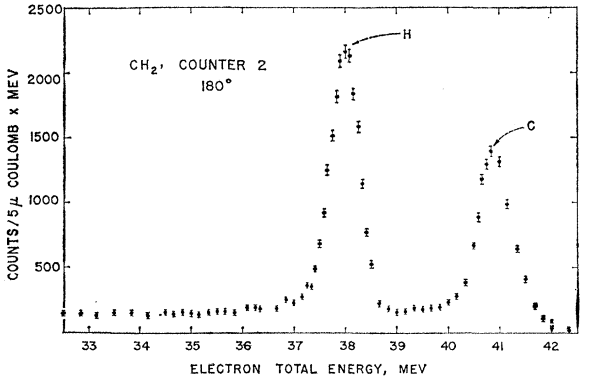

FIG. 4. Energy distribution of electrons, which were initially 41.5 MeV, after scattering through 180° from a CH_2 target.

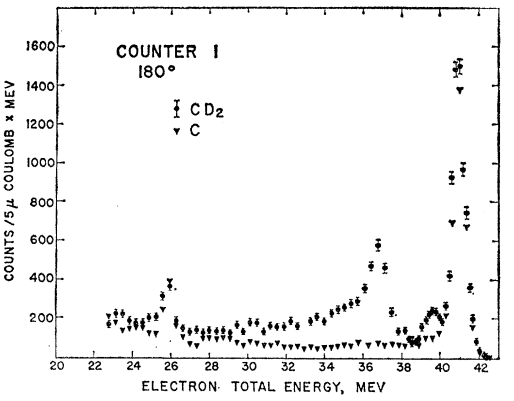

FIG. 5. Energy distribution of electrons, which were initially 41.5 MeV, after scattering through 180° from a CD_2 target.

area under the deuteron inelastic continuum to the area under the proton elastic peak for each counter. The standard deviation of the comparison for the three counter telescopes was 1.5%.

The constancy of effective solid angle with excitation energy was checked by measuring the carbon 15.1 MeV level with better statistics than are shown in Fig. 5. If the magnetic optics of the spectrometer-deflecting magnet combination were faulty, disagreement with 160° measurements[3] would be expected. No disagreement was found.

The data of the three counter telescopes were combined in proportion to the areas of their respective proton elastic peaks. This method of data combination tended to smooth out counting, monitoring, and background variations over the inelastic continuum because each of the three counter telescopes counted different energy electrons in the spectrum simultaneously. Greater confidence can be attached to the combined data of all counters than if the same total number of counts were accumulated on one counter.

IV. RADIATION CORRECTIONS

Radiation tails result mainly from two effects: (1) bremsstrahlung, either before or after the scattering event, in the electromagnetic field of another nucleus, and (2) the emission of quanta by the electron during the scattering event. These processes occur in both elastic and inelastic scattering.

A. Elastic Scattering

Sobottka[15,16] has included both of the above effects in finding a correction to elastic scattering. His result

[14] The larger size of the deuteron also tends to reduce the elastic scattering. We find a value of the spherically symmetric form factor, as defined by Jankus, of $f_D^2=0.77_{-0.10}^{+0.15}$ for $q=0.4\times10^{13}$ cm. This agrees with the Jankus calculation in which the nucleons in the deuteron are assumed to be point particles. This is a good approximation at the q values of this experiment.

[15] S. Sobottka, Stanford University, doctoral dissertation, 1960 (unpublished).

[16] Y. S. Tsai, Phys. Rev. 122, 1898 (1961). Radiation from the recoiling proton as well as the electron has been considered in this paper. However, for the energies of this experiment, Eq. (4) should be valid.

is based on the Bethe-Heitler[17] and the Schiff[18] bremsstrahlung formulations for the emission of hard and soft real and virtual quanta and is of the form:

Measured cross section
$$= (C) \times (\text{theoretical "bare" cross section}),$$
where

$$C=\frac{S+1}{\Gamma(1+y+y')}\left(\frac{E_0}{E_0'}\right)^{y}\left(\frac{\Delta E}{E_0'}\right)^{y+y'}\left\{1-\left(\frac{y}{1+y+y'}\right)\times\left(\frac{E_0}{E_0'}\right)^{2}(\Delta E)\left[\frac{1}{(d\sigma/d\Omega)}\frac{d}{dE}\left(\frac{d\sigma}{d\Omega}\right)\right]_{E_0}\right\}, \quad (4)$$

and

$$S=(2\alpha/\pi)(\ln\beta-\tfrac{1}{2}), \quad \beta=(\hbar c/mc^2)q,$$
$$y=x/0.739x_0+x'/0.739x_0'+S,$$
$$y=x/0.739x_0+x''/0.739x_0''+S.$$

x/x_0 is one-half the target thickness in radiation lengths; x'/x_0' and x''/x_0'' is the total thickness of all radiators before and after the target, respectively, such as monitor foils and windows, in radiation lengths; E_0 and E_0' are the electron's energy before and after scattering, respectively. $\Gamma(1+y+y')$ is the gamma function evaluated at $1+y+y'$.

We measured the area under the peak to the point where $\Delta E/E_0'$ was 0.03. This is sufficiently greater than the 0.01 fractional half-width of the main peak so that the structure of the main peak is not important in affecting the result.

The electron-proton scattering observed in this experiment is mainly due to an interaction between the electron and the magnetic moment of the proton. The Bethe-Heitler[17] and the Schiff[18] formulations describe the emission of radiation when an electron is accelerated in a Coulomb field. For want of a formulation for the radiation corrections to electron-magnetic moment scattering, it was assumed that the conditions set forth in their calculations were valid for this case.[19]

Sobottka's correction allows a comparison of an area under an elastic peak to a theoretical cross section, but it does not describe the shape of the radiation tail. The shape ordinarily can be described by expressions similar to those given by Barber *et al.*[3] The corrections for bremsstrahlung emission in the field of another nucleus either before or after the scattering event, is given by a sum of products of the bremsstrahlung and scattering cross sections. For a target composed of only one element,

$$\frac{d^2\sigma(E_0,E,\theta)}{d\Omega dE}=\frac{b(E_0,E')}{E_0-E'}t_i\frac{d\sigma}{d\Omega}(E',E,\theta)+\frac{b(E'',E)}{E''-E}t_s\frac{d\sigma}{d\Omega}(E_0,E'',\theta). \quad (5)$$

The first term describes the case where the electron radiates first and then scatters. Here, $b(E_0,E')/(E_0-E')$ is the bremsstrahlung number spectrum normalized to one radiation length for electrons of incident energy E_0 to produce photons of energy E_0-E' in a unit energy interval, t_i is half the target thickness plus the total thickness of other materials in front of the target (beam monitor foils and windows) expressed in radiation lengths, $(d\sigma/d\Omega)(E',E,\theta)$ is the elastic scattering cross section for the scattering of an electron incident with energy E' into a solid angle $d\Omega$ about θ giving a recoil energy $E'-E$ to the nucleus, the E is the electron energy measured. The second term describes the case where the electron scatters first and then radiates. Here, the nucleus recoils with energy E_0-E'' and t_s is half the target thickness plus the total thickness of other materials between the target and the spectrometer. This effect is proportional to the square of the target thickness.

For a target composed of two elements, there are eight possible sequences in which the electron radiates in the field of one nucleus and scatters in the field of another nucleus. In the case of CH_2, the proton and carbon cross sections, have different energy dependences and the recoil energies are different. This necessitates a detailed consideration rather than a simple CH_2-C subtraction. Equation (5) was evaluated for the eight cases and weighed according to the number of nuclei of each kind present in the target.

Contributions to the radiation tail resulting from radiation during the scattering event is described by a relation similar to that given by Friedman,[20] and is based upon the Schiff[18] result which treats the case where the electron has scattered through a large angle and photons are radiated in a small cone, either in the direction of the incident or the scattered electron.

$$\frac{d^2\sigma}{d\Omega dE}(E_0,E,\theta)=\frac{\alpha}{\pi}\left\{\left[\ln\left(\frac{2E_0}{mc^2}\sin(\theta/2)\right)-\frac{1}{2}\right]\right\}\times\left\{\left[\frac{1}{E_0-E_{0r}-E}\right]\left[1+\frac{E^2}{(E_0-E_{0r})^2}\right]\frac{d\sigma}{d\Omega}(E_0,\theta)+\left[\frac{1}{E_0-E-E_r}\right]\left[1+\frac{(E+E_r)^2}{E_0^2}\right]\frac{d\sigma}{d\Omega}(E+E_r,\theta)\right\}. \quad (6)$$

The first term within the second set of braces represents

[17] W. Heitler, *The Quantum Theory of Radiation* (Clarendon Press, Oxford, 1954), 3rd ed.
[18] L. I. Schiff, Phys. Rev. **87**, 750 (1952).
[19] Calculations by J. Schofield show the equivalence of the bremsstrahlung resulting from scattering in a Coulomb field or magnetic dipole field [J. Schofield (private communications)].
[20] J. I. Friedman, Phys. Rev. **116**, 1257 (1959).

the case of scattering first and then radiation, and the second term the opposite sequence. E_{0r} is the recoil energy given to a nucleus by an electron of initial energy E_0 that scatters elastically through an angle θ.

$$E_{0r}=\frac{2E_0^2\sin^2(\theta/2)}{Mc^2+2E_0\sin^2(\theta/2)}.$$

E_r is the recoil energy given to a nucleus by an electron that has final energy E upon elastic scattering.

$$E_r=\frac{2E^2\sin^2(\theta/2)}{Mc^2-2E\sin^2(\theta/2)}.$$

Both Eqs. (5) and (6) vanish for truly 180° electron scattering from spinless nuclei. McCormick, Keiffer, and Parzen[21] have integrated the Bethe-Heitler bremsstrahlung formula over all photon angles for a fixed electron scattering angle. They give an approximate formula for large electron scattering angles, and high electron energies, which for $\theta=180°$ reduces to

$$\frac{d^2\sigma}{d\Omega dE}(E_0,E)=\frac{\alpha Z^2}{8\pi}r_0^2\frac{m^2c^4}{(p_0c)^3}(1-\gamma-\gamma^{-1}+\gamma^{-2}), \quad (7)$$

where r_0 is the classical radius of the electron and $\gamma=p/p_0$. Thus, a radiation tail is expected at 180° for scattering from a spinless nucleus even though there is no elastic peak (in the approximation $m^2c^4/E_0^2\approx 0$).[12] Figure 6 shows a plot of the cross section as a function of γ.

The approach taken in the case of the proton was to add the radiation tail which always appears for 180° scattering, as given by Eq. (7), to the radiation tail associated with the elastic peak as computed from Eqs. (5) and (6). This approach gave results identical

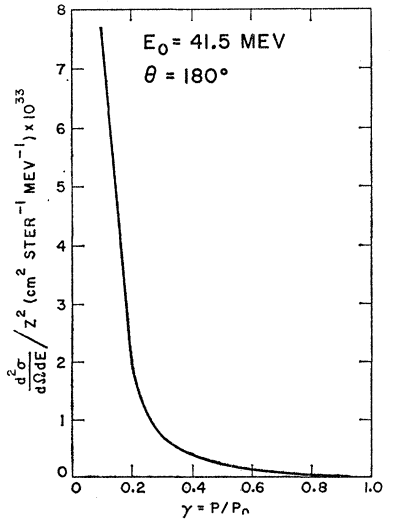

FIG. 6. Calculated radiation tail at 180° for a beam of 41.5-MeV electrons incident on a spinless nucleus.

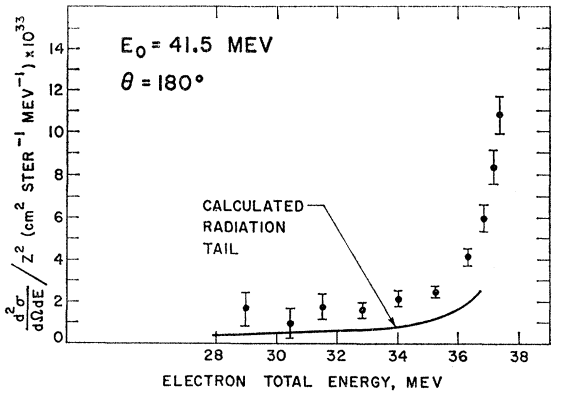

FIG. 7. Calculated and measured radiation tail at 177.1° for a beam of 41.5-MeV electrons incident on the proton. The calculated curve includes thick target effects.

to those obtained from the Berg-Lindner[22] formula for electron-proton bremsstrahlung in which we neglected the term involving interference between electron and proton bremsstrahlung. Other effects such as plural scattering and electron-electron scattering were found to give a negligible contribution.

Figure 7 shows the calculated and the measured radiation tail for the proton. Radiation during the scattering event accounts for 83% of the calculated radiation tail at $E=37$ MeV, and decreases to 67% at 28 MeV.

Clearly a large discrepancy exists between the proton radiation tail predicted by theory and the experimental data.

There are many experimental problems that could increase the measured radiation tail above that predicted by theory. For example, the discrepancy could be due to a low-energy beam contamination of bremsstrahlung and low-energy electrons, caused by the beam grazing some object before striking the target. To check this all components in the beam pipe were carefully aligned and realigned and a split-foil secondary-emission monitor was used to keep the beam centered. This effect also could give an additional charge collected by the secondary-emission monitor. This was not found to be the case. A contamination resulting from the beam striking the slit structure was unlikely because the entire structure was modified and the discrepancy still remained. The discrepancy probably did not result from the scattering of the electrons on the scattering chamber walls with concurrent ionization, radiation, and recoil energy losses, because the vacuum chamber was replaced with one of larger dimensions and no change in the scattering resulted. Also baffles and collimators were placed in various positions within the scattering chamber with no effect. A long vacuum tank having a thin entry window was placed between the pole pieces of the ditching magnet to eliminate the

[21] P. T. McCormick, D. G. Keiffer, and G. Parzen, Phys. Rev. **103**, 29 (1956).

[22] R. A. Berg and C. N. Lindner, Nuclear Phys. **26**, 259 (1961).

possibility of backscattering from the air, again with no effect upon the radiation tail.

If the radiation tail truly is larger than predicted by theory, there may be a number of theoretical uncertainties that may account for this. Among them are the uncertainties concerning wide angle bremsstrahlung in magnetic scattering, and the effect of nuclear size on bremsstrahlung.

B. Inelastic Scattering

Perez y Jorba[23] has extended the Schiff[18] calculation for elastic scattering to obtain radiation tail corrections for inelastic scattering for the case of emission during the scattering event. Perez y Jorba's result was modified, in the manner in which Friedman[20] modified Schiff's[18] expression, to allow for nuclear recoil, and the following equation, very similar to Eq. (6) was obtained:

$$\frac{d^2\sigma(E_0,\epsilon,E)}{d\Omega dE}=\frac{\alpha}{\pi}\left\{\left[\ln\frac{2E_0}{mc^2}\sin(\theta/2)-\frac{1}{2}\right]\right\}$$
$$\times\left\{\left[\frac{1}{(E_0-E_{0r}-\epsilon)-E}\right]\left[1+\frac{E^2}{(E_0-E_{0r}-\epsilon)^2}\right]\right.$$
$$\times\frac{d\sigma}{d\Omega}(E_0,E_0-E_{0r}-\epsilon)+\left[\frac{1}{E_0-(E+E_r+\epsilon)}\right]$$
$$\left.\times\left[1+\frac{(E+E_r+\epsilon)^2}{E_0^2}\right]\frac{d\sigma}{d\Omega}(E+E_r+\epsilon,E)\right\}.$$

$d\sigma(E_i,E_j)/d\Omega$ is the inelastic cross section for an electron which is incident with energy E_i and which leaves with energy E_j after exciting the nucleus to an energy ϵ above the ground state. Implicit in this equation is the assumption that the bremsstrahlung is predominately in the direction of the incident, or the scattered electron.

The radiation tail associated with the small deuteron elastic peak was subtracted from the inelastic continuum. The wide-angle bremsstrahlung contribution predicted by Eq. (7) is small except for energies far below the elastic peak. At $E=22$ MeV it is 15% of the total radiation tail.

The corrections for bremsstrahlung emission, either before or after the scattering event in the electromagnetic field of another nucleus, were made in a manner completely analogous to the treatment for elastic scattering.

The calculations were applied to the Jankus theoretical cross section as shown in Fig. 8 by treating the continuous inelastic spectrum as if it were made up of a finite number j of inelastic "levels" of excitation energies ϵ_j above the ground state. The radiation tails of these "levels" were added together to obtain the total radiation correction. The corrections at each "level" for electrons which have been removed to a lower level by radiation processes were modeled after proton elastic scattering corrections. The calculated proton elastic scattering is about 10% larger than the experimental elastic peak measured out to 3% from the elastic peak energy, according to the calculations of the previous section. A similar correction was made for each "level" for inelastic scattering. This correction is critical only near the inelastic peak. At lower energies, the main contribution comes from an accumulation of radiation tails from higher energy "levels."

[23] J. Perez y Jorba, J. phys. radium **22**, 773 (1961).

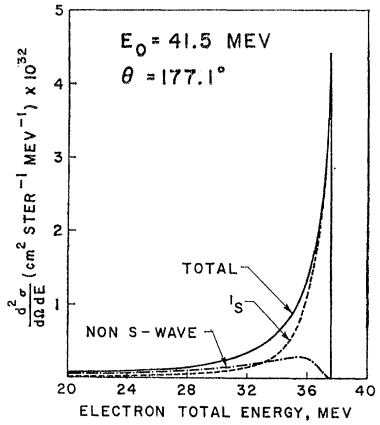

FIG. 8. Cross sections for the electrodisintegration of the deuteron by 41.5- MeV electrons scattered through 177.1° according to the theory of Jankus. The dashed curve labeled ^1S indicates the cross section for the $M1$ disintegration where the final state is ^1S. The dash-dot curve labeled *Non-S wave* indicates the sum of all cross sections for which the final states have angular momenta greater than zero. The solid curve labeled *Total* is the sum of these two cross sections.

V. COMPARISON WITH THEORY

The results are compared with the theory of Jankus,[6] which should give a reasonable description of deuteron electrodisintegration for the low momentum transfer conditions of this experiment. Jankus used the first Born approximation by considering the electron scattering process as a generator of Møller potentials which then act upon the deuteron's charge, current, and magnetization densities. Exchange currents were neglected and the nucleons of the deuteron were represented by point charges and point magnetic moments. Transition probabilities were computed for a pure triplet S ground-state wave function, which was a solution of the Hulthén potential, and for a final state plane wave function. By this means all multipole orders for the disintegration were included, but final state interactions were not taken into account.

For final S states, the interaction is very important and an explicit calculation was made for these cases. In the interests of analytical simplicity, the S-state wave functions were taken as solutions of Eckart potentials whose parameters were adjusted to give the

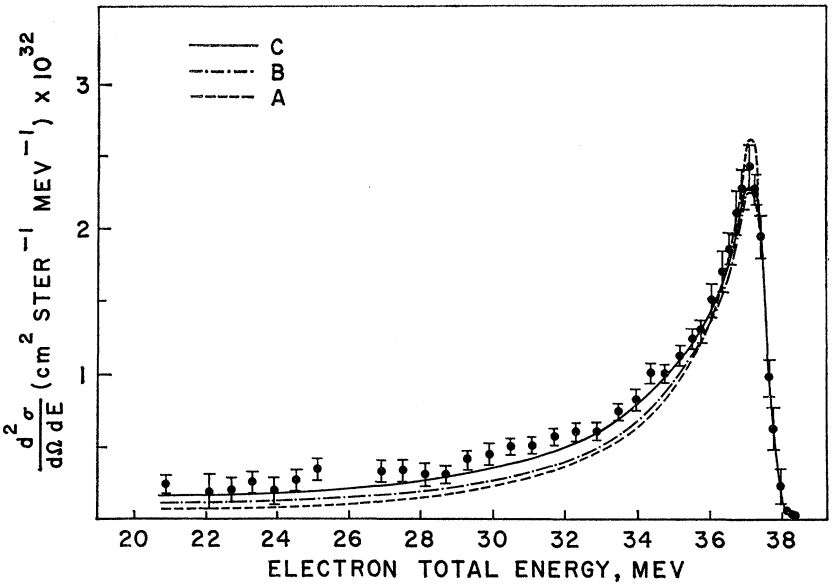

FIG. 9. Energy spectrum of 41.5-MeV electrons scattered inelastically through 177.1°. The dashed curve *A* and the dash-dot curve *B* represent the Jankus theoretical cross section folded by an experimental resolution function without and with radiation corrections, respectively. The solid curve *C* includes a preferred radiation correction obtained by multiplying the calculated radiation tails for inelastic scattering by the ratio of the measured to the calculated proton radiation tail.

values -23.8×10^{-13} cm for the singlet scattering length, 5.37×10^{-13} cm for the triplet scattering length, 2.63×10^{-13} cm for the singlet effective range, and 1.70×10^{-13} cm for the triplet effective range. The outgoing nucleons were treated nonrelativistically and interactions of the order of P^2/M^2c^2 were neglected, where P is the momentum of the outgoing nucleons.

Most of the assumptions of the theory are reasonable. For example, the neglect of the D state is unlikely to cause much error because the D state contribution enters directly, since interference effects between outgoing D and S waves average to zero for the case where none of the disintegration products are detected.

The use of a more realistic potential probably will not affect the results much for the excitation energies of this experiment. For example, the inclusion of a hard core of 0.42×10^{-13} cm in both the bound and unbound state[24] increases the $M1$ cross section only 4% for 16-MeV excitation, and even less for smaller excitations. The change in other contributions to the total cross section was less than one percent for 16-MeV excitation. However, at this excitation energy, the $M1$ cross section is quite sensitive to the value of the singlet effective range, even more so than the singlet n-p scattering cross section.[25,26] The uncertainty ($\sim$10%) associated with the singlet effective range, largely propagates to the $M1$ disintegration cross section for high excitation energies ($\sim$16 MeV), but is not as important for lower excitation energies. It would be desirable to recast the problem in the light of modern phenomenological potentials instead of matching to the effective-range theory.

The $M1$ cross section depends on currents due to nucleon and meson motions. Exchange currents, involving the detailed nature of the meson field, and arising in the theory from the introduction of a space exchange operator in the nucleon-nucleon coupling, enter in determining the shape and magnitude of the $M1$ cross section. Such effects are not important for low energy deuteron $E1$ disintegration since Siegert's theorem[27,28] is valid for electric multipole transitions, but not for magnetic multipole transitions.

There are features of the nuclear interaction, including exchange, which affect the ground state magnetic moment.[29,30] These "interaction effects" are manifest in various nuclear phenomena, such as the nonadditivity of spin and orbital magnetic moments in H^3 and He^3, and in thermal n-p capture cross sections.[30,31] In the latter case, the interaction effect gives about a 10% increase to the theoretical cross section predicted from a theory involving only the initial and final nucleon wave functions and the free nucleon moments. The effects of the nuclear interaction on the ground-state magnetic moment of the deuteron should appear as equivalent effects in the magnetic dipole transition probability.[29] Although detailed numerical estimates are not justified from the theory, it can be said that they are expected to be 10% or larger and probably become more important as the excitation energy increases.[32]

Figure 8 shows the Jankus[6] theoretical cross section for incident electrons of 41.5 MeV which are scattered into a solid angle $d\Omega$ about 177.1°. The magnetic dipole disintegration cross section is denoted by ^1S and

[24] H. W. Kendall, J. I. Friedman, E. F. Erickson, and P. A. M. Gram, Phys. Rev. 124, 1596 (1961).
[25] H. Bethe and C. Longmire, Phys. Rev. 77, 647 (1950).
[26] H. Feshbach and J. Schwinger, Phys. Rev. 84, 194 (1951).
[27] A. J. F. Siegert, Phys. Rev. 52, 787 (1937).
[28] L. D. Pearlstein and A. Klein, Phys. Rev. 118, 193 (1960).
[29] N. Austern and R. G. Sachs, Phys. Rev. 81, 710 (1951).
[30] N. Austern and E. Rost, Phys. Rev. 117, 1506 (1960).
[31] A. R. Baker and D. H. Wilkinson, Phil. Mag. 3, 647 (1958).
[32] J. M. Berger, Phys. Rev. 94, 1698 (1954).

TABLE I. Percentage difference between experiment and theory with modified radiation corrections.

Excitation interval (MeV)	1–4	4–7	7–11	12–17
$\left(\frac{\text{Experiment}-\text{Theory}}{\text{Theory}}\right)\times 100$	5.5	18	29	35
$M1$ percentage of total cross section	85	44	33	22

includes only the spin-flip transition $^3S_1 \rightarrow {}^1S_0$. The curve labeled "non-S wave" is the sum of all cross sections for which the final state has an angular momentum greater than zero.

After the theoretical cross section was corrected for radiation effects, as outlined in the previous section, it was then folded by a resolution function obtained from the shape of the proton elastic peak. This shape was governed by the momentum spread of the incident beam, aberrations in the focusing properties of the spectrometer, the momentum acceptance of the counter telescopes, ionization energy losses, and Landau straggling in the target. It was assumed that these features were independent of the energy of the scattered electron. The choice of resolution function is critical only near the peak of the inelastic spectrum, where the cross section varies rapidly with energy. The curves of Fig. 9 labeled A and B represent the Jankus theoretical cross section folded by the resolution function without and with radiation corrections, respectively.

TABLE II. Estimated percentage errors.

Source	Excitation energy 1 MeV	16 MeV
Incident beam energy	0	0
Angle of scattering	0	1
Target nonuniformity	2	2
Counter efficiency	1	2
Variation of solid angle	0	5
Proton cross section	4	4
Total error in percent	7	14

If the calculated radiation corrections are accepted, most of the experimental points are at least one standard deviation higher than the theory. However, as was pointed out in the previous section, there is good reason to believe that the radiation corrections should be larger than those calculated. The calculated radiation tail for the proton clearly is too small. If there are anomalous radiation effects for the far backward angles of this experiment, it is likely that they appear in the electrodisintegration of the deuteron as well as in elastic scattering from the proton. Also, if there are experimental reasons for the discrepancy in the proton radiation tail, they likewise will affect the deuteron radiation tail. For these reasons, we prefer a modified radiation correction. The curve of Fig. 9 labeled C was obtained by multiplying the calculated radiation tails for inelastic scattering from the deuteron by the ratio of the measured proton radiation tail to the calculated proton radiation tail, and adding the results to the Jankus electrodisintegration theory.

Even this modified radiation correction does not give agreement between experiment and theory. Table I gives the average percentage difference between the experimental points and the theory with modified radiation corrections for several energy intervals. Also the $M1$ percentage of the total cross section is indicated. It is unlikely that systematic errors should give rise to this disagreement. Table II gives estimates of possible sources of systematic errors.

The disagreement between theory and experiment might be explained by exchange effects, but a better radiation correction and a better theory of deuteron electrodisintegration is required before a quantitative determination of the contribution of exchange effects can be made.

ACKNOWLEDGMENTS

We are indebted to J. Carson who assisted throughout the course of the measurements, to E. Erickson for the use of a computer program for some of the theory, and to F. Bumiller and M. Yearian for several suggestions.